

Examining pressure-induced phase transformations in silicon by spherical indentation and Raman spectroscopy: A statistical study

Tom Juliano, Vladislav Domnich, and Yury Gogotsi^{a)}

A.J. Drexel Nanotechnology Institute and Department of Materials Science and Engineering, Drexel University, Philadelphia, Pennsylvania 19104

(Received 28 April 2004; accepted 23 July 2004)

Unloading rate and maximum load have been previously shown to affect the response of silicon to sharp indentation, but no such study exists for spherical indentation. In this work, a statistical analysis of over 1900 indentations made with a 13.5- μm radius spherical indenter on a single-crystal silicon wafer over a range of loads (25–700 mN) and loading/unloading rates (1–30 mN/s) is presented. The location of “pop-in” and “pop-out” events, most likely due to pressure-induced phase transformations, is noted, as well as pressures at which they occur. Multiple occurrences of pop-in and pop-out events are reported. Raman micro-spectroscopy shows a higher intensity of metastable silicon phases at some depth under the surface of the residual impression, where the highest shear stresses are present. A stability range for Si-II is demonstrated and compared with previous results for Berkovich indentation.

I. INTRODUCTION

It is known from high-pressure studies that silicon exhibits a phase transition from cubic diamond (Si-I) into a metallic β -tin structure (Si-II) in the pressure range of 9–16 GPa,^{1,2} accompanied with approximately 20% material densification. Under slow decompression from Si-II, the first phase to form at 10–12 GPa is Si-XII (or $r8$, rhombohedral structure with 8 atoms per unit cell),^{3,4} leading to 9% material expansion. On further pressure release, the degree of rhombohedral distortion diminishes gradually, producing a mixture of Si-XII and Si-III phases ($bc8$, body-centered cubic structure with 16 atoms per unit cell),^{3–5} with Si-XII persisting to ambient pressure.

Extensive experimental evidence suggests that single-crystal silicon undergoes similar phase transformations during indentation^{6–15} with the only difference being that the transformation path from Si-II is sensitive to unloading rate, producing mostly amorphous material (a-Si) under rapid unloading and the mixture of Si-III and Si-XII only when sufficient time is allowed for nucleation of these crystalline phases. Because the Si-I to Si-II transition is accompanied by sudden densification of the material underneath the indenter, it is believed to be evidenced in the indentation loading curve produced using a spherical indenter as a sudden displacement discontinuity

referred to commonly as a “pop-in” event [see Fig. 1(a)]. In support of this notion is the strong correlation between the pop-in pressure and the Si-I to Si-II transformation pressure as measured in high-pressure cell experiments.^{16,17} However, association of pop-in events with the onset of Si-I to Si-II phase transition was disputed recently by Bradby et al.,¹⁴ who suggested that phase transformation begins at earlier stages of loading and the pop-in is simply a manifestation of a sudden extrusion of highly plastic transformed material from underneath the indenter.

There is agreement in the literature that upon unloading, the formation of Si-XII is evidenced by “pop-out” or “kink pop-out” events, resulting from a sudden material expansion due to Si-I to Si-XII transformation, and the gradual amorphization of Si-II is evidenced by the “elbow” shape of the unloading curve, as illustrated in Fig. 1(b).^{11,14,18} This is supported by the results of phase characterization within the residual indents, carried out primarily by means of Raman spectroscopy^{6,11,18} and transmission electron microscopy (TEM).^{8–10,12,13,15}

It has been found for both Berkovich¹⁸ and spherical¹⁶ indentation that the maximum indentation load influences the transformation pressure of Si-II to Si-XII and Si-III. A greater maximum load will yield a greater transformation pressure upon unloading. Moreover, this transformation can be seen for a range of spherical indenter radii.¹⁷ For a larger radius tool, one must use a higher load to cause transformations in silicon, so that sufficient transformation pressure is built up underneath the tool.

In this work, for the first time an extensive statistical

^{a)}Address all correspondence to this author.

e-mail: gogotsi@drexel.edu
DOI: 10.1557/JMR.2004.0403

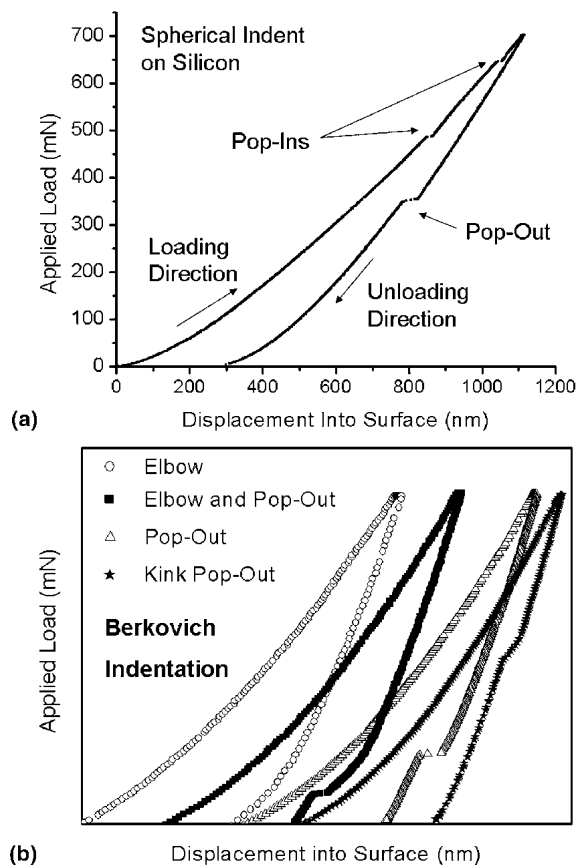


FIG. 1. (a) Load–displacement curve for a typical silicon indent, illustrating common curve features (maximum load of 700 mN, loading/unloading rate of 5 mN/s) and (b) indentation unloading curve shapes encountered for Berkovich indentation. Curves in (b) occur for different maximum loads, so each has been scaled to fit the figure.

study was done with a spherical indenter to find the response of silicon to a range of maximum loads (25–700 mN) and loading and unloading rates (1–30 mN/s). The pressures at which events in the loading and unloading curves occur (pop-in, pop-out and kink pop-out shapes) have been found and are compared to previous results obtained with a Berkovich indenter.¹⁸ Raman micro-spectroscopy was used to detect the presence of phases on and beneath the indented surface.

II. EXPERIMENTAL

A Nano Indenter XP (MTS Systems, Knoxville, TN) created all indentations at ambient conditions and continuously monitored load and displacement measurements during loading and unloading. The data collection rate was 5 Hz. Square arrays of indentations (7×7) were created for each tested parameter on the surface of the same polished *p*-type (111) silicon wafer, 1 mm thick. Indentations were spaced either 20 or 30 μm apart,

depending on maximum load. Each indentation was made with a sphero-conical diamond indenter with a 90° included angle and effective tip radius of 13.5 μm . The radius value was determined by calibration on a fused silica standard. An area function was fit by plotting the contact area over a range of contact depths from about 100–1500 nm. A total of 39 arrays and 1911 indentations comprised the data set. Each array contained indentations identical in terms of maximum applied load, loading rate, and unloading rate. For this work, loading rate and unloading rate were set to be the same value. Arrays for maximum applied loads of 25, 50, 75, 100, and 150 mN were made with loading/unloading rates of 2, 5, and 10 mN/s. Arrays for maximum applied loads of 200, 300, 500, and 700 mN were made with loading/unloading rates of 1, 2, 5, 10, 20, and 30 mN/s. For all experiments, the holding time at maximum load was 10 s.

After the indentations were made, a Ramascope 1000 Raman micro-spectrometer (Renishaw Inc., Gloucestershire, UK) was used to identify phases in the residual impressions. Over 100 indentations were checked using both the 514.5-nm wavelength of a green argon ion laser and the 633-nm wavelength of a red helium-neon laser. The motivation behind using two different wavelengths was to detect the amount of phases present at different depths beneath the indents. The 514.5-nm wavelength penetrates a Si-I surface about 800 nm, and the 633-nm wavelength, about 3 μm .¹⁹ However, signal absorbance for a-Si and other silicon phases are much greater,²⁰ so under the indented area penetration depths are expected to be much smaller. Collection times for each spectrum were 30 s. Lasers were focused through a $100\times$ optical objective so the spot size had a diameter of about 1–2 μm .

A Philips/FEI XL 30 field emission scanning electron microscope (SEM; Phillips International, Inc., Bethell, WA) was used to examine the morphology for a number of indents that exhibited different events in the loading and unloading curves. Typical operating voltages were between 3 and 10 KV. The sample was not cleaned or sputtered after indentations were made, to insure that all features created by the indenter remained intact.

To determine the average contact pressure during the first loading pop-in, purely elastic theory was used.²¹ This was deemed a valid assumption because indentations at loads just below this point of pop-in regularly showed completely elastic unloading. The average contact pressure is taken to be

$$\sigma_{\text{indentation}} = \frac{P}{\pi a^2}, \quad (1)$$

where P is the maximum applied load and a is the radius of contact between the indenter and the material. The maximum contact pressure will be at the center of the indent and is equal to $3/2$ the average contact pressure.

To determine the value of a for completely elastic loading, the following expression may be used^{21,22}

$$a = \sqrt{Rh - \frac{h^2}{4}} \quad (2)$$

where R is the indenter radius and h is the total measured displacement into the surface. This equation is based on the assumption that elastic contact depth is approximated by $h/2$. For the case of a second or third pop-in, Eq. (2) is no longer valid.

During unloading, a different approach must be used to find the pressure, based on analysis done by Iwashita et al and references therein.²³ A schematic illustrating some of the variables used is shown in Fig. 2. This time, the elastic and plastic response is taken into account. First, the elastic penetration depth of the material during loading is found by using the equation

$$h_e = \left(\frac{3P}{4E^*}\right)^{2/3} \left(\frac{1}{R}\right)^{1/3} \quad (3)$$

where E^* is the reduced modulus of the material, defined implicitly as

$$\frac{1}{E^*} = \frac{1 - \nu^2}{E} + \frac{1 - \nu_i^2}{E_i} \quad (4)$$

where ν and E are Poisson's ratio and elastic modulus for the indented material (silicon in this case), and the subscript i refers to the indenter properties. For these experiments, the values of ν , E , ν_i and E_i were taken as 0.2, 155 GPa, 0.07, and 1170 GPa, respectively. Silicon properties were determined experimentally.

The next step is to determine the penetration contact depth by taking into account the plastic portion. Contact depth can be found by

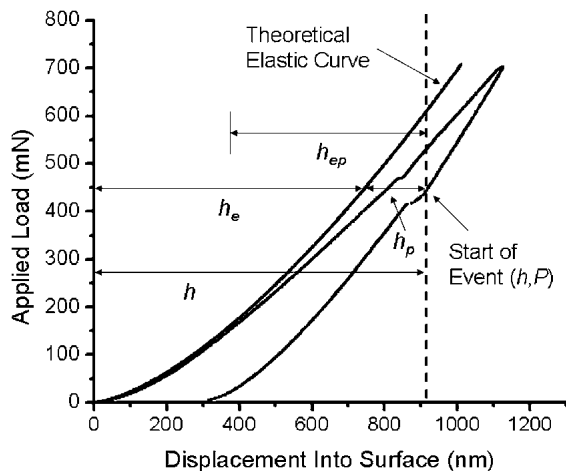


FIG. 2. Load–displacement curve illustrating parameters used to calculate event pressure during unloading. Purely plastic depth is given by h_p .

$$h_c = h - \frac{h_e}{2} \quad (5)$$

Finally, the radius of contact may be determined by the relation

$$a = \sqrt{2Rh_c - h_c^2} \quad (6)$$

and contact pressure at the point of the event given by Eq. (1). It is important to note that the average contact pressure defined by Eq. (1) bears no information on the stress tensor components, and therefore no attempt is made to assess the actual values of hydrostatic pressure and shear stress during indentation. Another limitation of this analysis is that the effect of cracking, which is seen at higher loads, is not taken into account. Cracking is expected to relieve stresses in the indented material so calculated pressure would be overestimated. However, it is expected that cracks will not largely influence the percentage of contact area and thus the value of calculated average contact pressure.

III. RESULTS AND DISCUSSION

A. Classification of indentation curves

All load–displacement curves were carefully examined after the tests. It was found that for the range of conditions tested, the only events during loading were pop-ins [Fig. 3(a)], and during unloading, pop-out [Fig. 3(b)] and kink pop-out [Fig. 3(c)] existed. Otherwise, during unloading, no event could be detected [Fig. 3(d)]. Formation of an elbow event frequently observed in Berkovich indentation¹⁸ was not observed. The pop-in is seen as a transient discontinuity on loading, the pop-out as a sudden flattening of the unloading curve and the kink pop-out as a spline-shaped unloading event.

These three events were characterized and detected by making use of numerical derivative analysis that utilizes a least-squares fit of nearby data points.²⁴ An example of the segments containing these events and their corresponding derivative behavior is shown in Fig. 3. Derivative plots may differ in shape slightly as more or less adjacent data points are taken into account. The initial pop-in can be detected readily from examining the derivative behavior [Fig. 3(a)]. Pop-out and kink pop-out shapes yield similar derivative shapes; however the kink pop-out derivative value minimum is not nearly as low as that for the pop-out (approximately 0.5 mN/nm compared to approximately 0.1–0.2 mN/nm). In this way, the two events can be separated. Another characteristic distinguishing the two is the number of data points that comprise the event for the same maximum load and loading/unloading rate, with the pop-out containing much less.

By the above analysis, each curve was characterized

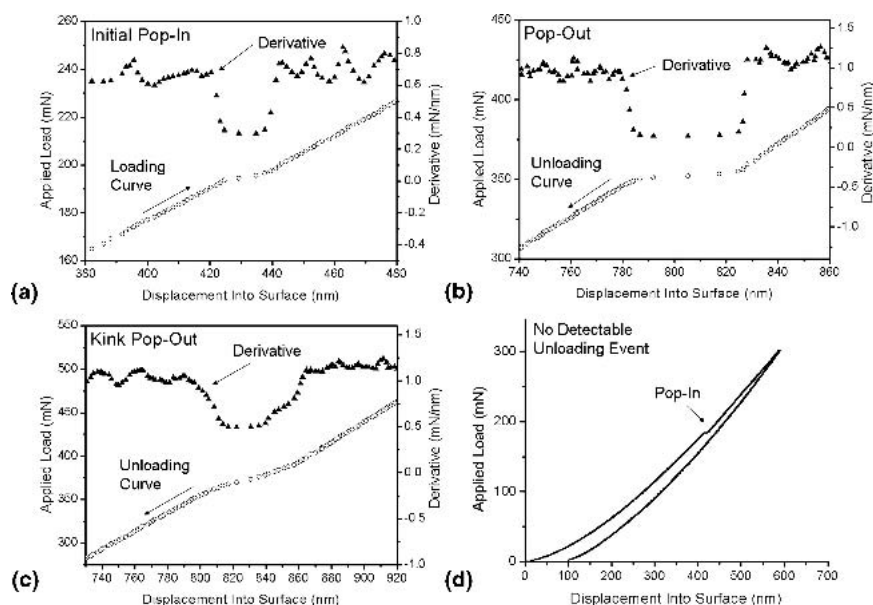


FIG. 3. Load–displacement and derivative behavior for (a) a pop-in event, (b) a pop-out event, (c) a kink pop-out event, and (d) no detectable unloading event.

by its unloading behavior and if the distinctive behavior was seen, classified as “pop-out” or “kink pop-out.” Many curves showed no detectable unloading events. For an event, the pressure was taken at the location where the derivative behavior begins to deviate from normal behavior.

B. Single and multiple pop-ins

The pressure of the initial point of pop-in was calculated for each indentation. A histogram showing the mean pressure between the indenter and sample for the beginning of pop-in is shown in Fig. 4. Event pressures are in a tight range for quick (30 mN/s) and slow (1 mN/s) loading, so it is reasoned that little or no dependence exists between initial pop-in pressure and loading rate in the range tested. Also, it was found that a

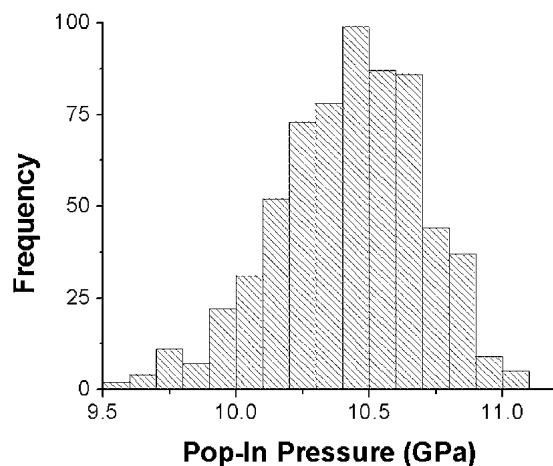


FIG. 4. Histogram of initial pop-in pressures for all indentations.

detectable pop-in event did not necessitate an unloading event, and vice versa. Because these events have been found to first appear near pressures Si-II forms in a diamond anvil cell (DAC), the histogram may be a measure of the upper stability range for Si-I, above which transformation to Si-II occurs.

A number of indents, especially those at maximum applied loads of 500 and 700 mN, showed multiple occurrences of pop-in phenomena (Fig. 1). Events after the initial pop-in are referred to as “subsequent pop-ins” here. To the authors’ knowledge, such a phenomenon in silicon has never been reported before. Initially, it was suspected that these events were due to material cracking on the surface. A number of indents were examined by SEM and matched with their respective load–displacement curves. Two examples of indents at a maximum load of 700 mN are shown in Fig. 5. Note the very irregular morphology inside the indented regions. It can be seen in Fig. 5(a) that although two major subsequent pop-ins occur, there is no obvious cracking around the indentation. In Fig. 5(b), there is only one major subsequent pop-in but three major cracks on the surface. Other examined indentations showed no correlation as well. Therefore, it is reasoned that the cause of these subsequent pop-ins is not cracking on the surface.

It has been considered that these events could be due to either subsurface cracking,²⁵ squeezing out of ductile material,¹⁴ or sudden dislocation bursts.^{26,27} Subsurface cracking may be possible but it would be dependent on the wafer orientation. As an example, indenting orthogonal to the (111) plane will promote formation of subsurface cracks. Further studies on different orientations should be carried out to determine this. For squeezing out

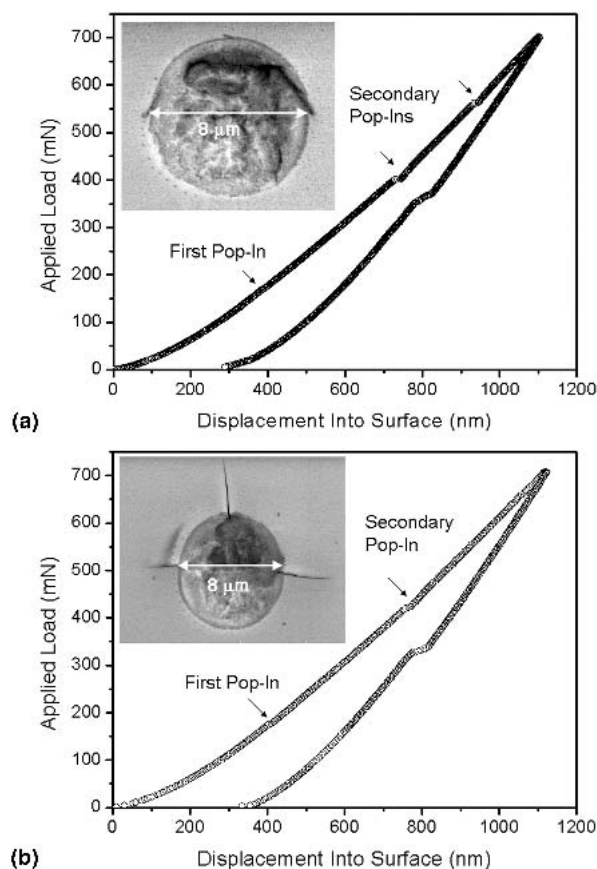


FIG. 5. Load–displacement curves and corresponding SEM micrographs for 700-mN indents showing (a) two secondary pop-ins for 1 mN/s loading/unloading rate and (b) one secondary pop-in for 5 mN/s loading/unloading rate. These events cannot be correlated with major cracks on the surface.

of ductile material, it appears likely that a noticeable amount would be found around the indented region, but none can be seen in the SEM. By contrast, a recent silicon indentation study performed using pyramidal indenters with varying included angles²⁸ showed that plastically extruded material was always observed for indentations with the axis-to-face angle of the tip less than 55°. However, no one-to-one correspondence was found between the extrusions and the occasional observation of small discontinuities in the loading curves.²⁸ By comparison, a Berkovich indenter is about 65° and the spherical indenter angles are about 78–81° over the depth range used in this study. For different radius spheres, if the initial pop-in event or subsequent pop-in events were due to material extrusion, it would seem likely that the pressure at which they occur be different, but this is not the case. However, for spherical indentation the prospect of multiple pop-in events due to extrusion of material cannot be completely dismissed.

For dislocation burst, it has been reported for silicon that dislocations may²⁶ or may not²⁹ be observed before the first pop-in; however this fact may be due to the

radius of indenter used. Dislocation formation in silicon has so far shown only a small effect on the loading curve compared to other materials. Therefore, subsequent pop-ins may be due to phase transformation or any of the other aforementioned causes. Further in situ work must be done to either support or refute these possibilities.

C. Multiple unloading events

Especially for greater loads (500–700 mN) and lower unloading rates (1–2 mN/s), sometimes two and even three events could occur in the unloading curve. These events could be either kink or regular pop-outs, and an example of the load–displacement and derivative behavior for multiple events is shown in Fig. 6. It is hypothesized that this is evidence for the possibility of multiple independent nucleation sites for Si-III and Si-XII underneath the indenter, and that it is sensitive to unloading rate. Multiple sites for Si-III and Si-XII have also been identified by the current authors in DAC work using Raman spectroscopy. Such behavior has never been reported before; however most studies of pop-out behavior with a spherical indenter either have been performed with smaller radius indenters than were used for this study^{10,12,16,30} (1–8.5 μm radius indenters compared to 13.5 μm) or the unloading rate was not sufficiently slow.¹⁷ It is likely that the smaller radius indenters simply do not produce enough area for multiple nucleation sites. As an example, for a 1-μm elastic penetration depth, a 3-μm radius tool will contact a 19-μm² area, while a 13.5-μm tool will contact an 85-μm² area, about 4.5 times greater than the 3-μm tool.

Because these events were mostly observed at lower unloading rates, 9 indents were made with a maximum applied load of 500 mN and unloading times of 5, 33, and 100 min to see the dependence. Out of the 9 indents, for unloading times of 5, 33, and 100 min, 0, 4, and 6 curves, respectively, showed multiple events in the unloading curve. Subsequently, it was confirmed that the likelihood of multiple unloading events increases as unloading time

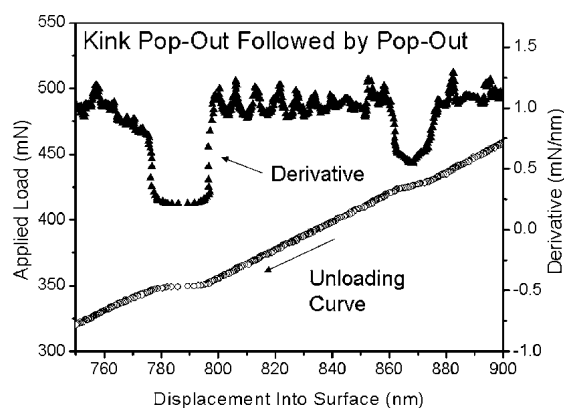


FIG. 6. Load–displacement and derivative data for two kink pop-outs.

increases when maximum load is sufficient. A number of indents showing multiple unloading events were examined with SEM and compared to those showing only single unloading events. No difference in the surface morphology could be detected. To confirm separate phase-changed areas underneath the indent, cross-sectional TEM should be used.

Separate phase-transformed regions might be due to multiple tip asperities common in larger-radius indenters. No such multiple asperities could be found on the tip using SEM, but they still may exist and help cause multiple pop-outs. On the particular tip used, perhaps there are asperities that could be of similar height, so only very slow unloading rates would accentuate the small height difference.

D. Raman spectroscopy

A number of curves with different combinations of loading and unloading events (i.e., pop-in, no unloading event; no pop-in, unloading event) were inspected with both 514.5- and 633-nm lasers to obtain phase profiles at different depths. A general trend was that a greater amount of a-Si, Si-III, or Si-XII is at deeper rather than shallower depths for a number of unloading conditions. The amount of these depths is likely in the range of 100–200 nm, based on absorbance values for a-Si.¹⁹ This can be determined by comparing relative heights of peaks belonging to phases other than Si-I to the Si-I 520 cm^{-1} peak. Sometimes, a strong a-Si signal without other phases could be found at more shallow depths, and a mixture of a-Si, Si-III and Si-XII at deeper depths. An example of Raman spectra for the same location on an indent with the two wavelengths is shown in Fig. 7(a) for formation of primarily Si-III and Si-XII, and in Fig. 7(b) for primarily a-Si. Note the variance in peak height relative to the normalized 520 cm^{-1} peak. Comparison with Berkovich indentation shows that the observed difference in Raman peak intensities is not due to resonance band enhancement of certain phases caused by different excitation wavelengths. In the case of sharp indenters, a higher intensity of metastable silicon phases was observed when 514.5-nm laser excitation was used. It may seem counterintuitive that a greater amount of transformed material would be at a greater depth. This may be related to the stress fields beneath the indenter, as explained below. Although the maximum stresses in the z direction (perpendicular to the sample surface) and radial (r) direction (perpendicular and intersecting with indenter axis of symmetry) occur on the surface of the indent, shear stress (τ_{zr}) along the z/r directions is maximum at a depth of $0.78a$, and equal to $0.2\sigma_{\text{indentation}}$. Figure 7(c) shows the profile of this shear stress as a function of z , a , and r for elastic, isotropic contact.²¹ It has been demonstrated that introducing shear stresses can

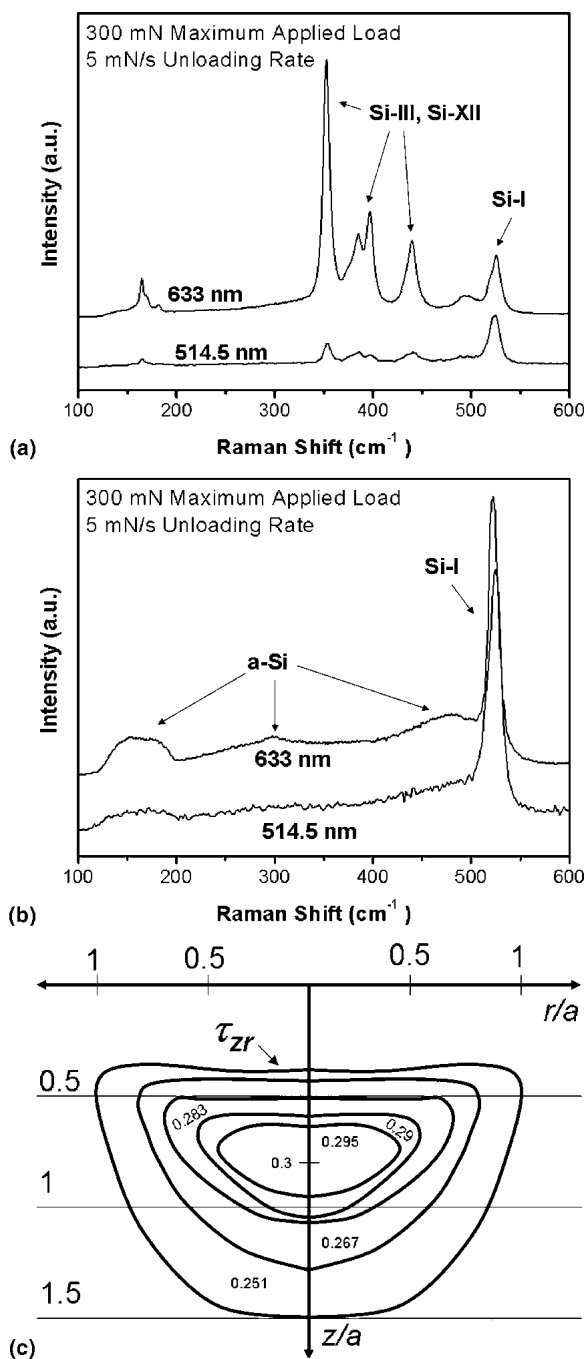


FIG. 7. (a) Raman spectra illustrating the variance of Si-III and Si-XII and (b) a-Si phase amounts found at two different depths beneath a 300-mN indent, and (c) shear stress contours underneath the indent, in units of maximum axial stress, p_o (after Ref. 18).

greatly lower pressures needed to initiate phase transformation of silicon and other semiconductors, compared with purely hydrostatic compression.^{31,32} For the case of the 300-mN indent shown in Fig. 7(a), at maximum load the maximum τ_{zr} would be 3.8 GPa at a depth of 220 nm beneath the surface. Although this amount of shear stress gives only an approximate value since phase transformation, cracking, and anisotropy exist, qualitatively it can

explain why most transformed material is observed at a comparably deeper depth underneath the sample surface for the case of a spherical indenter.

Raman results could not unambiguously demonstrate that a-Si, Si-III, and Si-XII phase changes are dependent on the events in the loading and unloading curves. When no detectable pop-in event was found, phase changes beneath the surface either could or could not be found for different indents. It was found that often the 520 cm^{-1} peak was shifted greatly to positions corresponding to as much as 4 GPa of residual stress,^{33,34} a magnitude not found for Berkovich indentation. If there was no detectable unloading event, sometimes metastable phases were found and other times they were not. This nullifies the claim that an absence of unloading curve events in silicon necessarily means that no phase transformation takes place in the indented region³⁵ and suggests that phase transformation can occur gradually during the loading or unloading process. Some spectra were taken multiple times in the same location to verify this.

Two consistent observations were made, however. First, if a detectable pop-out event occurred in the unloading curve, there was always some presence of Si-III and Si-XII phases as detected by the 633-nm wavelength laser. Second, if primarily amorphous material was detected, there was seldom a detectable unloading event, but if so, it was a very weak kink pop-out at a low pressure. Therefore, it can be reasoned that similar to Berkovich indentation,¹⁸ the pop-out and kink pop-out events are due mostly to formation of Si-III and Si-XII, with a possibility for a-Si formation as well. Likewise, “elbowing” shows evidence of a-Si formation, although the elbows in this study are much subtler and cannot be detected by normal means, unlike the case for Berkovich indentation. This may not hold true, though, for different, smaller radius indenters. It is reasonable to conclude that for curves showing no evidence of an unloading event, formation of amorphous material or other Si phases occur throughout a large portion of the unloading curve, at least for the parameters used.

E. Statistics of events for different unloading conditions

The number of unloading events that occurred varied greatly as a function of maximum load and unloading rate (Fig. 8). From Figs. 8(a) and 8(b), it can be discerned that for all conditions an unloading event did not always occur, since each array contained 49 total indents. Below 200 mN (or mean contact pressure of less than 10 GPa), no unloading curve events were seen at all. After pressures for each unloading event were determined, averages and standard deviations were plotted for each of the events (Fig. 9). In the Fig. 9 plots, averages for conditions with a small number of events (5 or fewer) are not shown.

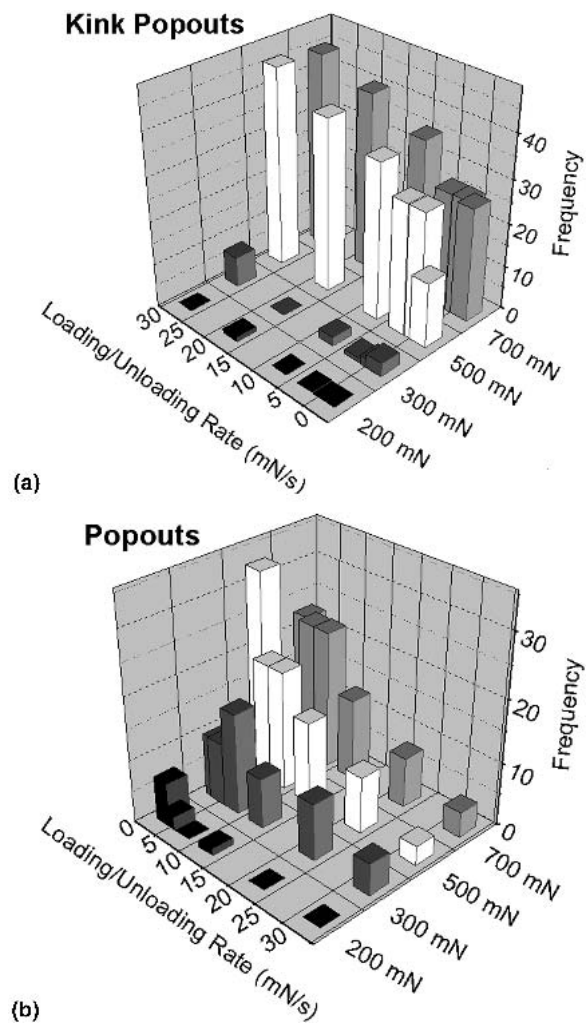


FIG. 8. Total events (out of 49 possible) for range of tested unloading conditions for the (a) kink pop-out and (b) pop-out unloading events.

As unloading rate decreases and maximum applied load increases, there is generally a greater chance of seeing pop-out and kink pop-out events. Because these events are caused by Si-III and Si-XII formation, such conditions favor formation of these phases. Therefore, amorphous material formation would have a higher probability of occurring with quicker unloading rates and lower loads. For the 200- and 300-mN indents, it was found via Raman spectroscopy that a number of indents did show strong a-Si peaks, unlike those with maximum applied loads of 500 and 700 mN. This trend is consistent with results for Berkovich indentation,¹⁸ where a-Si was not generally found underneath the indented area for higher applied loads, as compared to smaller ones.

From Fig. 9, both kink pop-out and pop-out pressures have a tendency to decrease as unloading rate increases, and as maximum applied load decreases. The same case happens for Berkovich indentation.¹⁸ This trend can be explained by considering the kinetics of the transformation and amount of transformed material underneath the

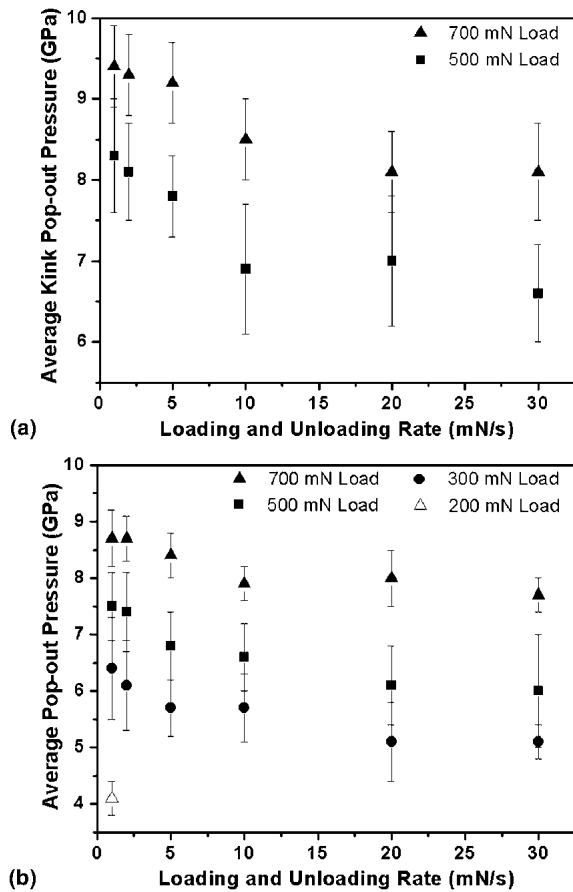


FIG. 9. Average event pressure for different maximum applied loads for the (a) kink pop-out and (b) pop-out unloading events.

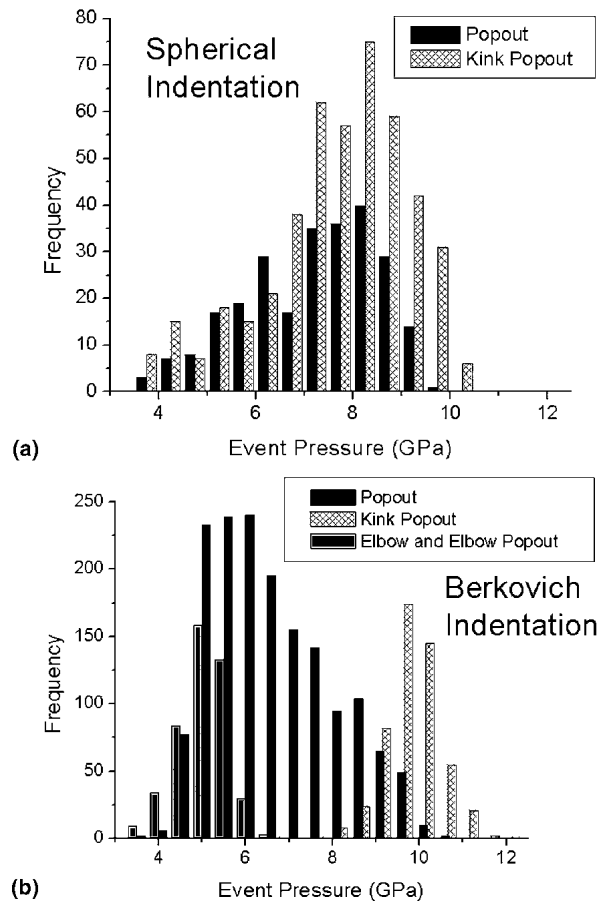


FIG. 10. Comprehensive frequency of event pressures for (a) the current spherical study and (b) the Berkovich study of Ref. 9.

indenter. When the tool is unloaded more quickly, the material has less time to change into another ordered phase, so then does so at a later time, or lower pressure. As more load is applied to the tool, a larger region is under transformation pressure underneath the tool. The greater the amount of constrained Si-II underneath the tool, the more thermodynamically unstable it is and will thus transform much sooner.

Figure 10(a) shows a histogram illustrating the pressure range over which all unloading events occurred for the indentations in this study. Figure 10(b) is a comparison of a similar histogram for a large number of Berkovich indentations with different maximum loads and unloading conditions, reproduced from Ref. 9. Some noteworthy observations proceed. First, the overall pressure range that events could occur is similar (approximately 3.5–12 GPa), while two different approaches to the pressure calculation were used for the sharp and spherical indentations. Second, the type of separation that kink pop-outs and pop-outs have from each other for Berkovich indentation does not seem to exist for spherical indentation. For the spherical histogram shown, it

could be argued that the pop-out and kink pop-out could be grouped together. However, in both cases the kink pop-out pressures tend to be higher than pop-out pressures. Third, kink pop-out events for Berkovich indentation tended to be at higher pressures than for spherical. This may be due to the high amount of shear stress found under a sharp indenter as compared with a spherical indenter. As noted earlier, shear stress can play an important role in aiding transformations in silicon. Alternately, as mentioned, cracking around indents would tend to overestimate transformation pressure values. Last, pop-out events occurred at similar ranges, while the kink pop-out pressure range for spherical indentation is much broader compared to Berkovich. This fact is evidence that Si-II is much more stable under generated pressure conditions of spherical indentation as compared to Berkovich, since the kink pop-out shape implies a more “sluggish” (longer time period) transformation of material than the pop-out shape. This may be due to the transformation zone being located under the surface and constrained by non-transformed Si-I from all sides, which can maintain a high residual stress during unloading.

IV. CONCLUSIONS

It has been shown that depth-sensing indentation and Raman micro-spectroscopy can give great insight into the response of silicon to contact loading induced by a spherical indenter. Spherical indentation done over a range of maximum applied loads and unloading rates reveals the stability of Si-I to be between 0 and 10.5 GPa and transformation to Si-II beginning at the upper bounds of this range. Si-II remains stable upon unloading to pressures between 3.5 and 12 GPa. This was discerned by taking into account the elasto-plastic behavior of silicon, compared with purely elastic theory. Multiple pop-ins and pop-outs on silicon have been reported; the cause of the pop-ins is not clear at this time, but the pop-outs were reasoned to be due to phase transformation. Raman spectroscopy demonstrated its ability to detect phase changes beneath the surface, giving different phase signature at different signal depths. The differences may be due in part to shear stresses helping to assist the transformation, although cross-sectional TEM studies should be performed to verify this. Unlike Berkovich indentation, phases could be found in the residual imprint when no unloading curve events could be detected. However, phases were always present in the indented region when an unloading event was found. Pressure ranges for kink pop-out events differed for Berkovich and spherical indentation, indicating that Si-II is generally more stable underneath the spherical contact encountered in the study. Finally, the overall stability range of Si-II is in general agreement for both Berkovich and spherical indentation, with the entire data set consisting of over 4500 indentations.

ACKNOWLEDGMENTS

The authors would like to thank Mr. A. Murugaiah for his useful input on pressure analysis and Mr. D. Ge for his ideas contributing to the paper. T.J. was supported in this work by a National Defense Science and Engineering Graduate Fellowship. This work was partly supported by National Science Foundation (NSF) Grant No. DMR-0116645 to purchase the Raman spectrometer. The SEM was funded through NSF Award No. BES-0216343.

REFERENCES

- J.C. Jamieson: Crystal structures at high pressures of metallic modifications of silicon and germanium. *Science* **139**, 762 (1963).
- J.Z. Hu, L.D. Merkle, C.S. Menoni, and I.L. Spain: Crystal data for high-pressure phases of silicon. *Phys. Rev. B* **34**, 4679 (1986).
- J. Crain, G.J. Ackland, J.R. Maclean, R.O. Piltz, P.D. Hatton, and G.S. Pawley: Reversible pressure-induced structural transitions between metastable phases of silicon. *Phys. Rev. B* **50**, 13043 (1994).
- R.O. Piltz, J.R. Maclean, S.J. Clark, G.J. Ackland, P.D. Hatton, and J. Crain: Structure and properties of silicon XII: A complex tetrahedrally bonded phase. *Phys. Rev. B* **52**, 4072 (1995).
- R.H. Wentorf and J.S. Kasper: Two new forms of silicon. *Science* **139**, 338 (1963).
- A. Kailer, Y.G. Gogotsi, and K.G. Nickel: Phase transformations of silicon caused by contact loading. *J. Appl. Phys.* **81**, 3057 (1997).
- J.S. Williams, Y. Chen, J. Wong-Leung, A. Kerr, and M.V. Swain: Ultra-micro-indentation of silicon and compound semiconductors with spherical indenters. *J. Mater. Res.* **14**, 2338 (1999).
- I. Zarudi and L.C. Zhang: Structure changes in mono-crystalline silicon subjected to indentation - experimental findings. *Tribol. Int.* **32**, 701 (1999).
- A.B. Mann, D. van Heerden, J.B. Pethica, and T.P. Weihs: Size-dependent phase transformations during point loading of silicon. *J. Mater. Res.* **15**, 1754 (2000).
- J.E. Bradby, J.S. Williams, J. Wong-Leung, M.V. Swain, and P. Munroe: Transmission electron microscopy observation of deformation microstructure under spherical indentation in silicon. *Appl. Phys. Lett.* **77**, 3749 (2000).
- V. Domnich, Y. Gogotsi, and S. Dub: Effect of phase transformations on the shape of the unloading curve in the nanoindentation of silicon. *Appl. Phys. Lett.* **76**, 2214 (2000).
- J.E. Bradby, J.S. Williams, J. Wong-Leung, M.V. Swain, and P. Munroe: Mechanical deformation in silicon by micro-indentation. *J. Mater. Res.* **16**, 1500 (2001).
- D. Ge, V. Domnich, and Y. Gogotsi: High-resolution transmission-electron-microscopy study of metastable silicon phases produced by nanoindentation. *J. Appl. Phys.* **93**, 2418 (2003).
- J.E. Bradby, J.S. Williams, and M.V. Swain: *In situ* electrical characterization of phase transformations in Si during indentation. *Phys. Rev. B* **67**, 085205 (2003).
- I. Zarudi, J. Zou, and L.C. Zhang: Microstructures of phases in indented silicon: A high resolution characterization. *Appl. Phys. Lett.* **82**, 874 (2003).
- E.R. Weppelmann, J.S. Field, and M.V. Swain: Observation, analysis and simulation of the hysteresis of silicon using ultra-micro-indentation with spherical indenters. *J. Mater. Res.* **8**, 830 (1993).
- E.R. Weppelmann, J.S. Field, and M.V. Swain: Influence of spherical indenter radius on the indentation-induced transformation behavior of silicon. *J. Mater. Sci.* **30**, 2455 (1995).
- T. Juliano, V. Domnich, and Y. Gogotsi: The effect of indentation loading conditions on the phase transformation induced events in silicon. *J. Mater. Res.* **18**, 1192 (2003).
- D.E. Aspnes and A.A. Studna: Dielectric functions and optical properties of Si, Ge, GaP, GaAs, GaSb, InP, InAs, and InSb from 1.5 to 6.0 eV. *Phys. Rev. B* **27**, 985 (1983).
- D.E. Carlson and C.R. Wronski: *Amorphous Silicon Solar Cells in Amorphous Semiconductors* (Springer, New York, 1979), pp. 287–330.
- K.L. Johnson: *Contact Mechanics* (Cambridge University Press, Cambridge, U.K., 1985), p. 452.
- J.S. Field and M.V. Swain: A simple predictive model for spherical indentation. *J. Mater. Res.* **8**, 297 (1993).
- N. Iwashita, M. Swain, J.S. Field, N. Ohta, and S. Bitoh: Elasto-plastic deformation of glass-like carbons heat-treated at different temperatures. *Carbon* **39**, 1525 (2001).
- T. Juliano, V. Domnich, T. Buchheit, and Y. Gogotsi: Numerical derivative analysis of load-displacement curves in depth-sensing

- indentation. In *Mechanical Properties of Nanostructured Materials and Nanocomposites*, edited by I. Ovid'ko, C.S. Pande, R. Krishnamoorti, E. Lavernia, and G. Skandan (Mater. Res. Soc. Symp. Proc. **791**, Warrendale, PA, 2004), p. 191 (Q7.5.1-Q7.5.11).
25. R.W. Armstrong, A.W. Ruff, and H. Shin: Elastic, plastic and cracking indentation behavior of silicon crystals. *Mater. Sci. Eng., A* **209**, 91 (1996).
 26. J.E. Bradby, J.S. Williams, J. Wong-Leung, M.V. Swain, and P. Munroe: Mechanical deformation of crystalline silicon during nanoindentation, in *Fundamentals of Nanoindentation and Nanotribology II*, edited by S.P. Baker, R.F. Cook, S.G. Corcoran, and N.R. Moody (Mater. Res. Soc. Symp. Proc. **649**, Warrendale, PA, 2001), pp. Q8.10.1–Q8.10.6.
 27. H. Saka, A. Shimatani, M. Sukanuma, and Suprijadi: Transmission electron microscopy of amorphization and phase transformation beneath indents in Si. *Philos. Mag. A* **82**, 1971 (2002).
 28. G.M. Pharr, J.I. Jang, and S. Wen: Phase transformation and cracking in brittle materials during nanoindentation, presented at High Pressure Phase Transformations Workshop, University of North Carolina at Charlotte, NC, August 20, 2003.
 29. H.S. Leipner, D. Lorenz, A. Zeckzer, and P. Grau: Dislocation-related pop-in effect in gallium arsenide. *Phys. Status Solidi* **183**, R4 (2001).
 30. I. Zarudi, L. Zhang, and M. Swain: Behavior of monocrystalline silicon under cyclic microindentations with a spherical indenter. *Appl. Phys. Lett.* **82**, 1027 (2003).
 31. B.A. Galanov and V.M. Kindrachuk: Contact mechanics models accounting for phase transformations. In *High-Pressure Surface Science and Engineering* (Institute of Physics, Bristol, U.K., and Philadelphia, PA, 2004), pp. 21–56.
 32. J.J. Gilman: Shear-induced metallization. *Philos. Mag. B* **67**, 207 (1993).
 33. I. De Wolf: Micro-Raman spectroscopy to study local mechanical stress in silicon integrated circuits. *Semicond. Sci. Technol.* **11**, 139 (1996).
 34. G. Lucazeau and L. Abello: Micro-Raman analysis of residual stresses and phase transformations in crystalline silicon under micro-indentation. *J. Mater. Res.* **12**, 2262 (1997).
 35. A.V. Byakova, S.N. Dub, Y.V. Milman, N.A. Efimov, and A.A. Vlasov: *Structure and Mechanical Properties of Si-based Coatings* (E-MRS 2003 Spring Meeting Abstracts, Strasbourg, France, 2003).